Neural-based Iterative Approach for Iris Detection in Iris recognition systems

Ruggero Donida Labati, Vincenzo Piuri *Fellow, IEEE*, Fabio Scotti *Member, IEEE*

***Abstract*— The detection of the iris boundaries is considered in the literature as one of the most critical steps in the identification task of the iris recognition systems. In this paper we present an iterative approach to the detection of the iris center and boundaries by using neural networks. The proposed algorithm starts by an initial random point in the input image, then it processes a set of local image properties in a circular region of interest searching for the peculiar transition patterns of the iris boundaries. A trained neural network processes the parameters associated to the extracted boundaries and it estimates the offsets in the vertical and horizontal axis with respect to the estimated center. The coordinates of the starting point are then updated with the processed offsets. The steps are then iterated for a fixed number of epochs, producing an iterative refinements of the coordinates of the pupils center and its boundaries. Experiments showed that the method is feasible and it can be exploited even in non-ideal operative condition of iris recognition biometric systems.**

I. Introduction

THE detection of the pupil center is a complex and critical operation in iris recognition systems which can greatly influence the performance of the whole recognition system. Wrong estimations of the iris center and boundaries (the iris-pupil and iris-sclera intensity transitions) can produce the acquisition of unreliable iris features, and hence it can produce wrong identifications.

The recognition process is divisible in four distinct steps: acquisition of the biometric data, segmentation, feature extraction and matching. This paper focuses on the second step, which consists in the extraction of the iris area in the acquired image. Most of the times, algorithms approximate the iris and the pupil boundaries with two circumferences [1-6]. In this approach, a wrong estimation of the position of the centers of the circumferences can significantly worsen the result of this step. The feature extraction step consists in the generation of a template from the segmented image. In this step, most algorithms[1-3] linearize the circular iris pattern in a rectangular image, then they produce a template by applying 2D filters to the linearized image (for example e bidimensional wavelet filtering). Again, this operation requires a correct position of the pupil center. In literature there are many algorithms that performing the localization of the iris center and its boundaries [1-9].

Unfortunately, most of the presented methods are optimized in specific applicative setups and they tend to produce wrong behaviors in noisy and difficult applicative contexts with particular reference to the localization of the pupil center [7]. In [13], a neural-based approach to the segmentation of the iris pattern is presented where each single pixel of the input image is evaluated and classified as belonging or not to the iris pattern.

In this paper, we present a new method capable to find the iris center and the relative inner boundary from an input eye image. The proposed method is iterative, it starts from an initial random input point, and, for each iteration, it processes a candidate relative position of the pupil center. After each iteration, the method refines the center estimation unless the process is terminated. During each iteration, the method extracts from the input image a local circular portion, and it linearizes this portion by using a conversion from Cartesian to Polar coordinate system. In this new image space, a localization of the most probable iris boundary edges is processed by a derivative approach obtaining a vector of boundary points. The points dataset is then interpolated by a polynomial, and the processed coefficients are the inputs of two neural networks. Each neural network returns the estimated distance of the input point from the estimated pupil center along the x and y axis. This approach has been verified for 100 images in three different scenarios: input points inside of the pupil, input points inside of the iris and input points outside of the iris. Results are encouraging and they show that the method is feasible.

The paper is structured as follows. In the next section, the proposed approach is presented and detailed. In section III, the creation of Training and Test datasets is discussed, it is presented the creation of the neural networks and the overall results are given and compared with other techniques present in the literature. In the last section it is discussed the overall behavior of the proposed method and the future work.

II. The proposed approach

The proposed solution consists in an iterative algorithm which starts from a random point in the input image, and it aims to locate the center of the pupil through an iterative refining of the current position in the image. The proposed method is capable to analyze the local image property of the current image, in order to estimate the x and y directions toward the pupil center. When the current point is situated too far from the iris boundaries, the algorithm behavior is comparable to a random walk. Otherwise, when the input point is situated in the pupil area, the algorithm is capable to achieve a fine searching of the pupil center. As such, the expected behavior of the proposed approach can be seen as a explorative random walk capable to detect the pupil presence, and then to achieve a fine tuning of the center localization.

In the proposed method, each single iteration is partitioned in two distinct steps: (i) a local estimation of a set of image characteristics and (ii) an estimation of the pupil center

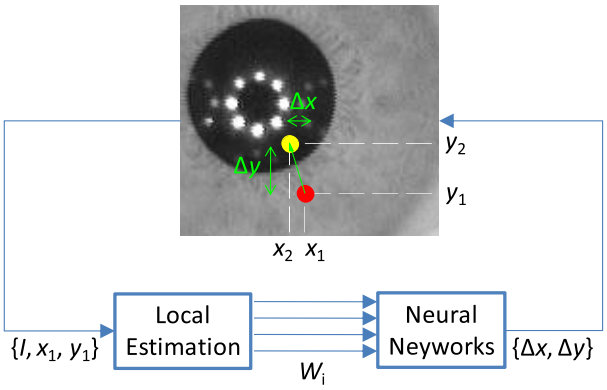

Fig. 1. Iterative algorithm schema.

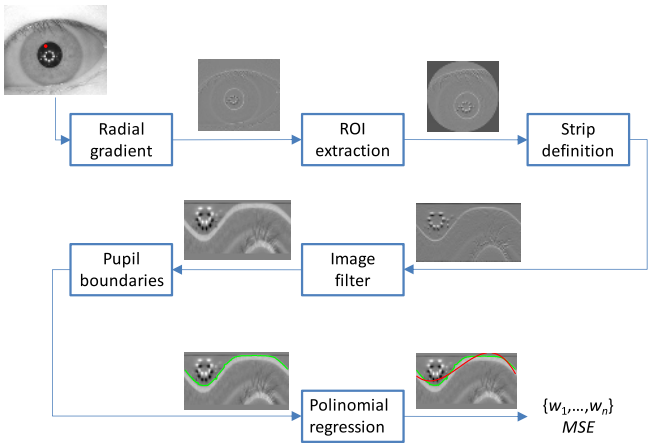

Fig. 2. Local estimation schema.

position with two artificial neural networks. Fig. 1 shows an application of the method. Starting from an initial point (x_1, y_1) of the image I, the method processes a set of image local properties (the parameters set W_i), and it estimates the corrective deltas along the x and y axis processed by means of two neural networks. The output point (x_2, y_2), where $x_2 = x_1 + \Delta x$, and $y_2 = y_1 + \Delta y$, will be used as starting point in the next iteration. A termination criterion is hence needed to stop the iterations when the center of the pupil has been found with sufficient accuracy, or in the case of erroneous convergence of the algorithm. Let us now detail all the steps of the proposed algorithm.

A. Local Estimation

The Local Estimation step (Fig. 2) extracts from the input image I a circular Region of Interest (ROI in the following) centered in the current point (x_1, y_1), then it extracts the available information concerning the circular transitions of the gray-level intensity which are eventually present in the ROI. In fact, these particular patterns are typically associated to the presence of the iris boundaries. The candidate boundary patterns are then fitted with a polynomial curve by a linear regression method. The outputs of the regression operation used in input to the neural networks are: (i) a set of coefficients of the approximated polynomial $(w_1, \ldots w_n)$ describing the inner iris boundary in the polar coordinates space, and (ii) the Mean Squared Error of the regression.
More in detail, we propose the following sequence of steps in order to extract the proper candidate boundary curve and the center of the iris:

1) the gradient of the original image in radial direction with respect to the input point (x_1, y_1) is processed;
2) a circular region of interest in the radial gradient image (ROI) of fixed radius and centered in (x_1, y_1) is produced by cropping the complete image;
3) a linearized strip image S is generated from the extracted ROI;
4) the stripe image is then filtered with an horizontal mean filter with a kernel size of $K \times 1$;
5) the points of the inner iris boundary in the image strip are estimated by processing each single column by a modified edge detector method, and then collecting the obtained vertical coordinate values in vector $Y = [y_1, \ldots y_C]$ where C are the available columns in the strip image;
6) the vertical coordinates in Y are then used for estimate by a linear regression method an approximated polynomial

$$\hat{Y} = w_0 + w_1 x + w_2 x^2 + \ldots w_D x^D \qquad (1)$$

where $x \in [1 : C]$, and D is the degree of the polynomial;
7) the mean square error of the regression is then processed

$$MSE = (1/n) \sum_{i=1}^{n} (y_i - \hat{y}_i)^2 \qquad (2)$$

and the parameters are then collected in the vector $W = [w_1, \ldots w_D, MSE]$.

A more detailed description of the methods used in the steps from 1) to 4) can be found in [8,10].
The localization of the inner iris boundaries (step 5) can be achieved by considering the fact that the transitions of the iris boundaries in the linearized gradient image correspond to bright horizontal objects in a noisy dark background as the effect of the mean filter (fifth subplot in Fig. 2). Hence, it is possible to locate the largest object in the strip S by a binarization approach, and then to process the vertical coordinates of the maximum intensities along each single column and storing them in the Y vector. In the following, we refer to the binarized image obtained from image S as image B. Further details will be given in the experimental section.

B. Neural networks

In this study, we use two different artificial neural networks to estimate the distance from the input point to the effective center along the x and the y axis. The inputs of the neural networks are the coefficients of the approximated iris boundaries W, as plotted in Fig. 3.

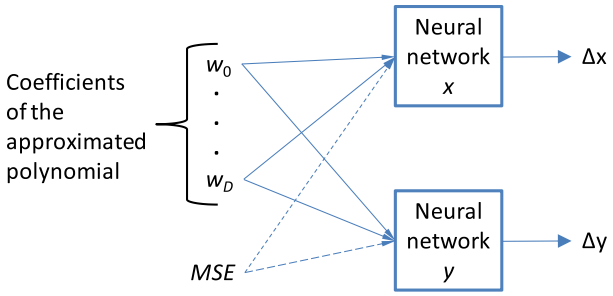

Fig. 3. Neural networks inputs and outputs.

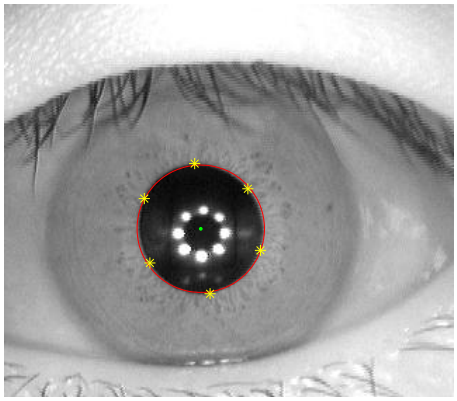

Fig. 4. Example of points used for train the neural networks: the true center is the central dot point and the six crosses are the data points used for compute its estimation.

The goal of the neural networks is to approximate two non-linear functions $\Delta_x = F_x(W)$ and $\Delta_y = F_y(W)$ capable to process the estimated local parameters W in order to obtain the required relative increments Δ_x and Δ_y of the current coordinates (x_1, y_1) needed to jump as close as possible to the iris center (Fig. 1).

In order to create a proper training and evaluation framework, we manually located the center of the pupils for a portion of a public dataset of iris image (the CASIA-IrisV3-Interval [11]). At the best of our knowledge, no public iris image dataset are available with the data regarding the iris center. Since the manual estimation of the pupil center is an hard and imprecise operation, we preferred to adopt a more robust method to obtain the positions of the pupil centers. We have manually selected N points from the pupil boundaries (this task is much easier for a user than the direct estimation of the center), and we applied a least square procedure to approximate the pupil boundaries points as a circumference. We consider as "true" the centers of the estimated circles for each image. Fig. 4 plots an example of the procedure that we used to estimate the centers in an image dataset. The crosses in the picture mark the six points chosen by the supervisor to estimate the center of the pupil (central dot). We created three different datasets depending on the position of the training points: (i) inside the pupil, (ii) inside the iris, (iii) outside the iris. The complete description of the datasets will be given in the next section.

C. Termination condition

The iteration of the proposed method can be terminated by different approaches. In this work we discuss the following two termination conditions:

1) the algorithm stops after a defined number of iterations;
2) the algorithm stops when the distance between the centers processed in two subsequent iterations is lower than a fixed value.

Further details concerning the termination condition will be given in the next section.

III. Experimental results

In this section we describe how the parameters of the Local Estimation step have been fixed, how we built the training and test datasets of the neural networks, and we propose a set of figure of merit that can be used to estimate the accuracy of the proposed algorithm.

A. Creation of the training and test datasets

The Local Estimation step of the proposed algorithm requires to fix four sets of parameters according the adopted image dataset. In our tests, we have used the following configuration of the parameters:

- the minimum and maximum radius of the circular ROI used to process the linearized stripe are equal to 2 pixel and 110 pixel respectively;
- the kernel size of the mean filter is $[21 \times 1]$ pixels;
- the binarized image B produced from image S (the linearized circular ROI) has its pixels equal to one if the corresponding pixels in S have a positive value and their intensity value greater than the 10% of the maximum intensity;
- for all objects present in B (we consider one object if it consists at least of an eight-connected pixel area of the image [11]) we use a subset composed by the 5 largest candidates, then the largest object along the horizontal axis is as most probable iris border transaction.

B. Creation of the training and test datasets

We created the training and test datasets by randomly selecting 100 images from the CASIA-IrisV3-Interval database [11]. From this subset of images we created four different datasets:

1) the first (dataset **A**) is composed by 1000 points selected inside the pupil area (10 points $\times$ 100 images);
2) the second (dataset **B**) is composed by 1000 points randomly selected inside the iris (10 points $\times$ 100 images);
3) the third (dataset **C**) is composed by 1000 points which have been randomly selected outside the iris area (10 points $\times$ 100 images);
4) the fourth (dataset **T**) is the training dataset for the neural networks and it is composed by dataset A plus the true center of each image (1100 points).

Fig. 5 plots the positions of the points belonging to the datasets A, B and C on the same example image.

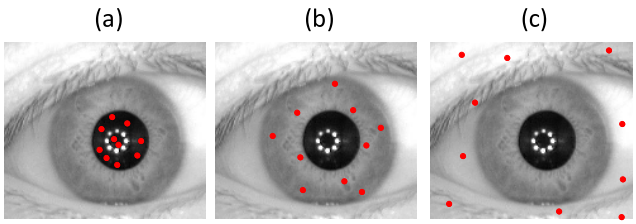

Fig. 5. Examples of selected points in the training and test dataset: (a) points in the pupil area belonging to the dataset A; (b) points in the iris area belonging to the dataset B; (c) points outside the iris boundaries belonging to the dataset C.

C. The neural networks training phase

In order to effectively estimate the generalization error of the trained neural networks, we adopted a simple two-fold cross validation technique: 50% of the available points of the dataset T have been used for the calibration of the parameters and for the training of the neural networks; the remaining 50% have been used only for the test/validation operations. The topology of the neural networks has been design as follows: we used a linear node for the output layer of the neural networks and we tested different configurations for the hidden layer. In particular, we have tested one and two layers with different topologies: log-sigmoidal and tan-sigmoidal.We trained the neural networks by using the back-propagation algorithm. Table I and II report the training and validation errors of the tested neural networks by using dataset T. These errors refer to the mean errors of the outputs Δ_x and Δ_y of the neural network in one single step of the proposed algorithm (Fig. 1).

TABLE I

TRAINING RESULTS FOR THE x NEURAL NETWORK

Polinomial order	Node topology	# of nodes in layer 1	# of nodes in layer 2	Trainig error	Validation error
3	log-sig	12	no	1,8739	2,0099
3	tan-sig	9	no	1,7796	1,9235
3	log-sig	10	7	1,8315	1,9057
3	tan-sig	8	5	1,8949	2,0264
2	log-sig	10	no	1,9055	1,9522
4	log-sig	8	no	1,8296	1,9873

TABLE II

TRAINING RESULTS FOR THE y NEURAL NETWORK

Polinomial order	Node topology	# of nodes in layer 1	# of nodes in layer 2	Trainig error	Validation error
3	log-sig	5	no	4,7499	3,6052
3	tan-sig	6	no	4,7455	3,6714
3	log-sig	5	3	4,6637	3,6062
3	tan-sig	5	4	5,0616	4,0271
2	log-sig	5	no	5,5826	4,5181
4	log-sig	5	no	5,1254	4,1845

Experiments demonstrated that the neural networks trained with dataset T are more accurate in validation then the neural network trained with dataset A.
Moreover, from these test results, it is possible to observe that the MSE index does not significantly influence the accuracy. This parameter can probably improve the results only if there is a systematic error in the linear regression step or in case of a wrong behavior of the approximation algorithm (for example reflections boundaries are included in the interpolation in spite of the real iris boundaries). We tested also different hidden layer configurations with no significant increment in accuracy.
Notably, the order of the approximant polynomial influences the accuracy. Results indicate that a simple order 3 polynomial is suitable to allow the neural network to correctly estimate the quantities Δ_x and Δ_y.

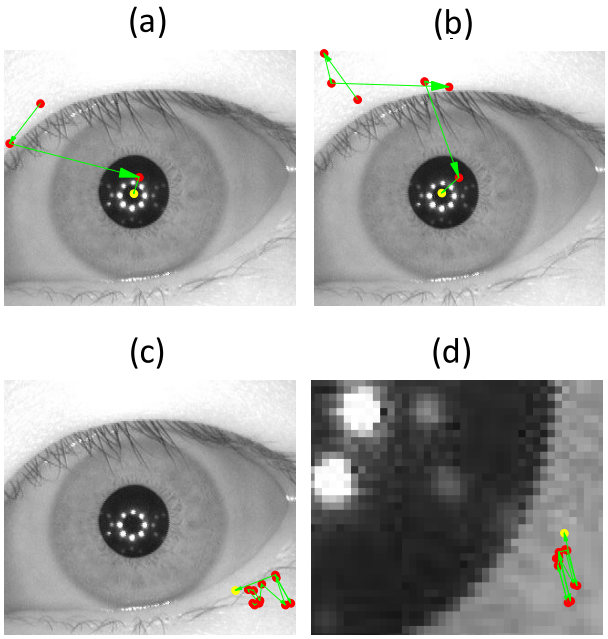

Fig. 6. Example of trajectories: in (a) and (b) the pupil center is correctly found; in (c) and (d) the algorithm does not work properly.

D. Final results of center localization

In general, the number of iterations of the algorithm is variable for each starting point. In fact, the number of iterations and the length of the displacements Δ_x and Δ_y depends on the local characteristics of the image. For instance, then the starting point is close to a iris area, the movements of the point are very short since it is needed only a fine tuning of the center position. Differently, if the starting point is next to the eyelashes, a failure of the algorithm is possible because the moving point can be attracted by them. Fig. 6 shows two examples of correct convergence of the method, and two situation when the points fall in a portion of the image different from the pupil.

The results of the algorithm are related to the adopted termination criterion. In our case, it is two-fold:

1) the iterations stop when the algorithm arrives to the maximum iteration number M;
2) the computation can perform an early-stop when, for two iterations, the displacements positions Δ_x and Δ_y have a distance minor then a fixed distance Δ_D measured in pixel.

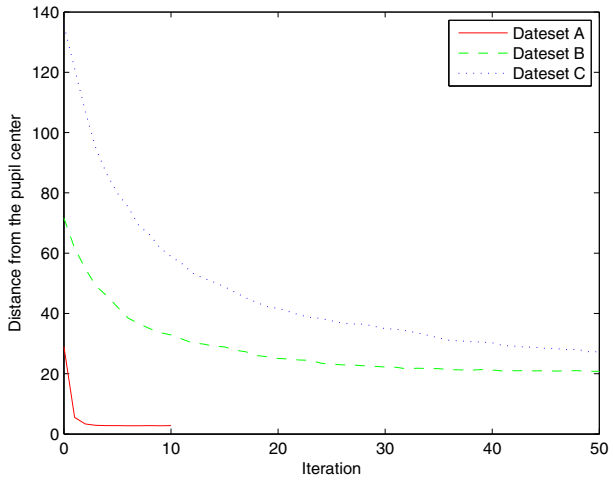

Fig. 7. Mean error obtained with the first termination criterion for the datasets A, B and C.

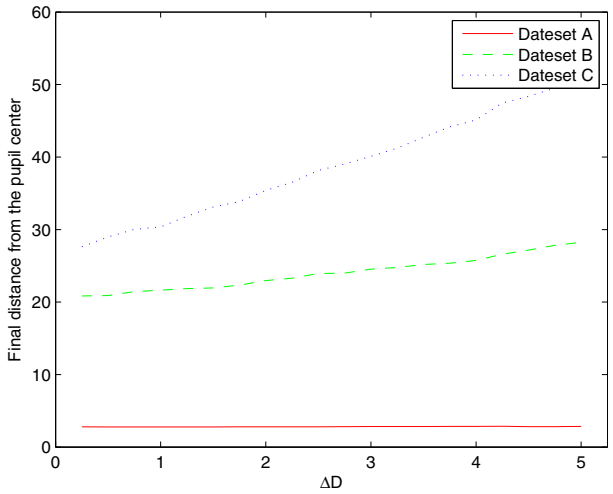

Fig. 8. Final mean error obtained with the second termination criterion for the datasets A, B and C.

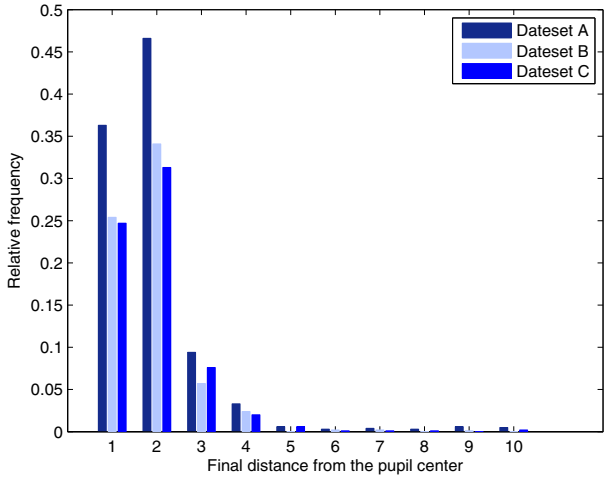

Fig. 9. Relative frequency of the different error distances, obtained with the first termination criterion. The parameter I is equal to 10, 50 and 50 respectively for the dataset A, B and C.

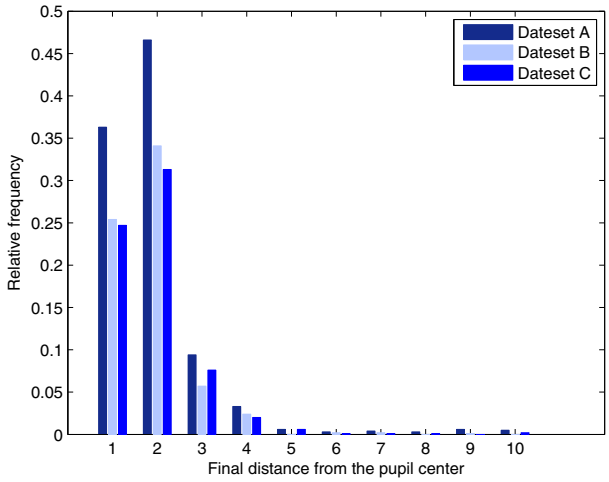

Fig. 10. Relative frequency of the different error distances, obtained with the second termination criterion. The parameter I is equal to 10, 50 and 50 respectively for the dataset A, B and C. The parameter Δ_D is equal to 1, 0.5 and 0.5.

The design of these two parameters (M, Δ_D) can be done for different datasets by observing the curves plotted in Fig. 7 and Fig. 8. In Fig. 7 it is plotted the average distance error of the algorithm over the dataset A, B, and C for each iteration. It can be seen that after 40-50 iterations there is not significant reduction of the error distance for the dataset A, B and C. Hence, a value of M equal to 50 is the adopted. Fig. 8 plots the error distance at the moment of the early stopping of the proposed method for different Δ_D. Notably, when the proposed algorithm is dealing with the harder datasets (like B and C) the early stopping criterion limits the final accuracy, but in the case of dataset A, this drawback is not present and the early stopping criterion can produce a significant reduction of the convergence time.

Notably, the simple analysis of the mean error distance is not sufficient to measure the accuracy of the proposed method, since two very different behaviors are present. When the algorithm correctly converges, the final error distances are very small. In the opposite case, the final position can be very far from the correct center and these error values strongly effect the mean error.

A more refined analysis can be done by considering the distribution of the errors of the proposed algorithm. The plots in Fig. 9 and in Fig. 10 show the relative frequency of the final error distance of the proposed algorithm. Results show that in most cases the final error is less than three pixels for all the datasets. The performances on dataset B and C are slightly worse. In fact, dataset B and C produce a minor percentage of final positions close to the real pupil center than the dataset A, since a larger number of points can ”trapped” in different areas of the image (like eyelashes or different circles), but the overall behavior is satisfactory.

We compared the proposed algorithm to different techniques available in the literature for locating the iris

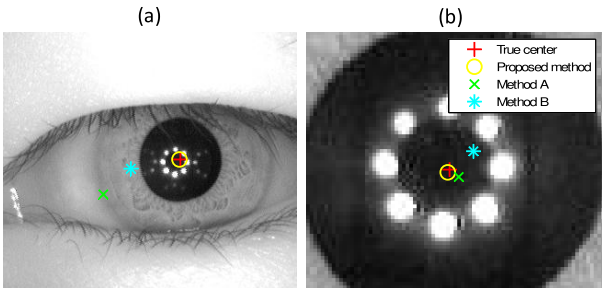

Fig. 11. Two examples of the estimated pupil center by the different algorithms.

center: the method based on the Hough operator [11] implemented by L. Masek [12] available in a public code library which has been optimized for the same images we used in all datasets (Method A), and a method based on the work of J. Daugman presented in [1]. These two methods was tested using the images employed to built the datasets A, B and C. The results obtained from the comparisons are resumed in Table III.

TABLE III
MEAN ERRORS

	Method A	Methot B	Proposed method		
			Dataset A	Dataset B	Dataset C
Error	31.9573	4.0827	2.761	20.7774	27.2612

In Table IV, we report the number of images where the pupil center was better located by the proposed approach with respect to the reference method A and B on the three datasets.

TABLE IV
NUMBER OF IMAGES WITH BETTER RESULTS THAN THE REFERENCE ALGORITHMS

	Proposed method		
	Dataset A	Dataset B	Dataset C
Method A	69%	17%	12%
Method B	70%	56%	53%

A qualitative analysis of the behavior of the proposed algorithm on two sample images can be found in Fig. 11. As shown in the reported results, the proposed algorithm works very well when it starts from a point situated close to iris/pupil (dataset A), but when the starting point belongs to other zones of the image, the obtained accuracy decreases. The reason of this behavior is not surprising since the proposed algorithm, in these areas, is comparable to a random walk. Future improvements are needed to solve this drawback which is essentially related to the strong dependence of the proposed algorithm on the random starting point. Preliminar experiments showed that this dependence can be strongly reduced by adopting an approach which encompasses several restarts of the algorithm with different starting points.

IV. CONCLUSION

The paper presented an iterative method capable to localize the iris in an eye image and to produce an accurate estimation of the center coordinates of the pupil. Starting from an initial random point in the image, the algorithm process the local property of the selected image region, and then estimates the displacement toward the iris center along the x and y axis by means of two trained neural networks. The two main steps of the algorithm are then repeated until the termination criterion is reached. The main drawback of the proposed algorithm is related to the strong dependence on the position of the initial starting point, but experiments showed that this dependence can be strongly reduced by adopting few restarts of the algorithm with different starting points. Experiments demonstrate that the method is feasible and it has a remarkable accuracy, also when applied in non ideal/noisy image types.

REFERENCES

[1] J. Daugman, "How iris recognition works," *Circuits and Systems for Video Technology, IEEE Transactions on*, vol. 14, no. 1, pp. 21–30, Jan. 2004.
[2] R. Wildes, "Iris recognition: an emerging biometric technology," *Proceedings of the IEEE*, vol. 85, no. 9, pp. 1348–1363, Sep 1997.
[3] W. Boles and B. Boashash, "A human identification technique using images of the iris and wavelet transform," *Signal Processing, IEEE Transactions on*, vol. 46, no. 4, pp. 1185–1188, Apr 1998.
[4] X. He and P. Shi, "A new segmentation approach for iris recognition based on hand-held capture device," *Pattern Recogn.*, vol. 40, no. 4, pp. 1326–1333, 2007.
[5] W. Kong and D. Zhang, "Accurate iris segmentation based on novel reflection and eyelash detection model," 2001, pp. 263–266.
[6] A. Ross and S. Shah, "Segmenting non-ideal irises using geodesic active contours," 19 2006-Aug. 21 2006, pp. 1–6.
[7] R. Donida Labati and F. Scotti, "Noisy iris segmentation with boundary regularization and reflections removal," *Image and Vision Computing, Iris Images Segmentation Special Issue*, On printing.
[8] J. Daugman, "New methods in iris recognition," *IEEE Transactions on Systems, Man, and Cybernetics, Part B*, vol. 37, no. 5, pp. 1167–1175, 2007.
[9] R. Ives, L. Kennell, R. Gaunt, and D. Etter, "Iris segmentation for recognition using local statistics," 28 - November 1, 2005, pp. 859–863.
[10] R. C. Gonzalez and R. E. Woods, *Digital Image Processing (3rd Edition)*. Upper Saddle River, NJ, USA: Prentice-Hall, Inc., 2006.
[11] C.B.S.R., Center for Biometrics and Security Research, http://www.cbsr.ia.ac.cn.
[12] L. Masek and P. Kovesi, 2003. MATLAB Source Code for a Biometric Identification System Based on Iris Patterns. The School of Computer Science and Software Engineering, The University of Western Australia.
[13] R. Broussard, L. Kennell, D. Soldan, and R. Ives, "Using artificial neural networks and feature saliency techniques for improved iris segmentation,"*Neural Networks, 2007. IJCNN 2007. International Joint Conference on*, Aug. 2007, pp. 1283–1288.